Genetic ablation of lymphocytes and cytokine signaling in nonobese diabetic mice prevents diet-induced obesity and insulin resistance

Randall H. Friedline,*[,1] Hwi Jin Ko,*[,1] Dae Young Jung,* Yongjin Lee,* Rita Bortell,*[,†] Sezin Dagdeviren,* Payal R. Patel,* Xiaodi Hu,* Kunikazu Inashima,* Caitlyn Kearns,* Nicholas Tsitsilianos,* Umber Shafiq,* Leonard D. Shultz,[‡] Ki Won Lee,[§] Dale L. Greiner,*[,†] and Jason K. Kim*[,§,¶,2]

*Program in Molecular Medicine, [†]Diabetes Center of Excellence, and [¶]Division of Endocrinology, Metabolism, and Diabetes, Department of Medicine, University of Massachusetts Medical School, Worcester, Massachusetts, USA; [‡]The Jackson Laboratory, Bar Harbor, Maine, USA; and [§]World Class University Biomodulation Major, Department of Agricultural Biotechnology and Center for Food and Bioconvergence, Seoul National University, Seoul, Republic of Korea

ABSTRACT   Obesity is characterized by a dysregulated immune system, which may causally associate with insulin resistance and type 2 diabetes. Despite widespread use of nonobese diabetic (NOD) mice, NOD with severe combined immunodeficiency (*scid*) mutation (SCID) mice, and SCID bearing a null mutation in the IL-2 common γ chain receptor (NSG) mice as animal models of human diseases including type 1 diabetes, the underlying metabolic effects of a genetically altered immune system are poorly understood. For this, we performed a comprehensive metabolic characterization of these mice fed chow or after 6 wk of a high-fat diet. We found that NOD mice had ~50% less fat mass and were 2-fold more insulin sensitive, as measured by hyperinsulinemic-euglycemic clamp, than C57BL/6 wild-type mice. SCID mice were also more insulin sensitive with increased muscle glucose metabolism and resistant to diet-induced obesity due to increased energy expenditure (~10%) and physical activity (~40%) as measured by metabolic cages. NSG mice were completely protected from diet-induced obesity and insulin resistance with significant increases in glucose metabolism in peripheral organs. Our findings demonstrate an important role of genetic background, lymphocytes, and cytokine signaling in diet-induced obesity and insulin resistance.—Friedline, R. H., Ko, H. J., Jung, D. Y., Lee, Y., Bortell, R., Dagdeviren, S., Patel, P. R., Hu, X., Inashima, K., Kearns, C., Tsitsilianos, N., Shafiq, U., Shultz, L. D., Lee, K. W., Greiner, D. L., Kim, J. K. Genetic ablation of lymphocytes and cytokine signaling in nonobese

The nonobese diabetic (NOD) mouse is an inbred mouse strain first reported in 1980 and has been widely used as the favored model to study the pathogenesis of autoimmune, T-cell–mediated type 1 diabetes in humans for >30 yr (1, 2). Mice homozygous for the severe combined immunodeficiency (*scid*) mutation are severely deficient in functional T and B lymphocytes (3), and NOD-*scid* (SCID) mice have been primarily used as recipients of diabetogenic NOD cells (4, 5) or as a mouse xenograft model to study multiple human diseases (6–8). The significance of these mouse models has recently amplified with their application in the development of humanized mice for the study of type 1 and type 2 diabetes (9). Despite such an important role and extensive and historical use of NOD and SCID mice by the diabetes research community, little is known about their metabolic states and their response to diet-induced obesity, a commonly used model of type 2 diabetes.

Obesity is a major cause of insulin resistance and type 2 diabetes (10), and recent studies have shown an important role of a dysregulated immune system in obesity-mediated insulin resistance (11–13). Obesity is characterized by altered levels of circulating cytokines, and adipose tissue macrophage infiltration and inflammation are causally associated with insulin resistance (14–16). Obesity-associated inflammation develops in multiple organs including skeletal muscle, a major organ of glucose disposal, and cytokine-mediated suppression of local inflammation

---

Abbreviations: 2-[^{14}C]DG, 2-deoxy-D-[1-^{14}C]glucose; HFD, high-fat diet; HGP, hepatic glucose production; NOD, nonobese diabetic; NOD-*scid*, nonobese diabetic with severe combined immunodeficiency mutation (SCID); NSG, NOD-*scid* bearing a null mutation in the IL-2 common γ chain receptor; *Rag1*, recombination activation gene 1; RER, respiratory exchange ratio *scid*, severe combined immunodeficiency; SCID, nonobese diabetic with severe combined immunodeficiency (NOD-*scid*); V_{CO_2}, carbon dioxide production; V_{O_2}, oxygen consumption; WT, wild-type

has been shown to ameliorate skeletal muscle insulin resistance (17, 18). Furthermore, mice lacking macrophages, cytokines, or lymphocytes have all been shown to exhibit alterations in glucose and lipid metabolism (19–21). Taken together, there is overwhelming evidence to support a primary and causal role of an altered immune system in obesity, insulin resistance, and type 2 diabetes.

Recently, SCID bearing a null mutation in the IL-2 common γ chain receptor (NSG; NOD-$scid$ $IL2R\gamma^{null}$) mice were generated and found to be a more appropriate animal recipient for xenograft transplantation studies (22, 23). NSG mice are deficient in mature lymphocytes and NK cells, and a recent study has found that NSG mice become obese in response to high-fat feeding but remain glucose tolerant (24). In our current study, we have carefully performed energy balance and metabolic studies in NOD, SCID, and NSG mice following a chow or high-fat diet (HFD) for various periods of time to determine the effects of underlying alterations in the immune system on glucose homeostasis.

MATERIALS AND METHODS

Animals and diet

Male NOD (NOD/LtJ), male lymphocyte-deficient SCID (bearing the $Prkdc^{scid}$ mutation; NOD.CB17-$Prkdc^{scid}$/J), male NSG (NOD.Cg-$Prkdc^{scid}$ Il2rg^{tm1Wjl}/SzJ), and male wild-type (WT; C57BL/6J) mice were obtained from The Jackson Laboratory (Bar Harbor, ME, USA). We used male C57BL/6J mice for comparison because this is the most commonly used background genetic strain for mice with altered metabolism and for the diabetes research community. Starting at 14 wk of age, mice were fed an HFD (TD 93075; 55% kcal from fat; Harlan Teklad, Indianapolis, IN, USA) ad $libitum$ for 5–12 wk as indicated in the text ($n = 6$–15 per group) or remained on a standard chow diet ($n = 5$–11 per group). All animal studies were approved by the Institutional Animal Care and Use Committee of the University of Massachusetts Medical School.

Body composition and energy balance

Whole-body fat and lean mass were noninvasively measured using ^{1}H-MRS (Echo Medical Systems, Houston, TX, USA). Indirect calorimetry and energy balance parameters including food/water intake, energy expenditure, respiratory exchange ratio (RER), and physical activity were noninvasively assessed for 3 d using metabolic cages (TSE Systems Inc., Chesterfield, MO, USA).

Hyperinsulinemic-euglycemic clamp

Following chow or an HFD, a survival surgery was performed at 5–6 d before clamp experiments to establish an indwelling catheter in the jugular vein. On the day of the clamp experiment, mice were unfed overnight (~15 h), and a 2 h hyperinsulinemic-euglycemic clamp was conducted in conscious mice with a primed and continuous infusion of human insulin [150 mU/kg body weight priming followed by 2.5 mU/kg per minute; Humulin (Eli Lilly and Company, Indianapolis, IN, USA)] (25). To maintain euglycemia, 20% glucose was infused at variable rates during clamps. Whole-body glucose turnover was assessed with a continuous infusion of [3-^{3}H]glucose (PerkinElmer, Waltham, MA, USA), and 2-deoxy-D-[1-^{14}C]glucose (2-[^{14}C]DG) was administered as a bolus (10 µCi) at 75 min after the start of clamps to measure insulin-stimulated glucose uptake in individual organs.

At the end of the clamps, mice were anesthetized with pentobarbital, and tissues were taken for biochemical analysis (25).

Biochemical analysis and calculation

Glucose concentrations during clamps were analyzed using 10 µl plasma by a glucose oxidase method on the Analox GM9 Analyzer (Analox Instruments Limited, Hammersmith, London, United Kingdom). Plasma concentrations of [3-^{3}H]glucose, 2-[^{14}C]DG, and ^{3}H$_2$O were determined following deproteinization of plasma samples as previously described (25). For the determination of tissue 2-[^{14}C]DG-6-phosphate content, tissue samples were homogenized, and the supernatants were subjected to an ion-exchange column to separate 2-[^{14}C]DG-6-phosphate from 2-[^{14}C]DG. Plasma insulin levels were measured using an ELISA kit (Alpco Diagnostics, Salem, NH, USA).

Rates of basal hepatic glucose production (HGP) and insulin-stimulated whole-body glucose turnover were determined as previously described (25). The insulin-stimulated rate of HGP was determined by subtracting the glucose infusion rate from whole-body glucose turnover. Whole-body glycolysis and glycogen plus lipid synthesis from glucose were calculated as previously described (25). Insulin-stimulated glucose uptake in individual tissues was assessed by determining the tissue (*e.g.*, skeletal muscle) content of 2-[^{14}C]DG-6-phosphate and plasma 2-[^{14}C]DG profile.

Statistical analyses

Data are expressed as mean ± SE values, and differences between groups were examined for statistical significance using the ANOVA with Fisher's exact test. A probability value of $P < 0.05$ was used as the criterion for statistical significance. All analyses were performed using Statistical Analysis Software (SAS Institute Inc., Cary, NC, USA). For metabolic experiments involving hyperinsulinemic-euglycemic clamps and multigroup comparison, 10 mice provide sufficient power (90%) to determine the changes in insulin sensitivity at >20% difference between the groups (~30% SD) with statistical significance at $P < 0.05$ level with 2-sided null hypothesis.

RESULTS

Basal metabolic phenotypes in chow-fed mice

At 5 mo of age, body weights were comparable among WT, NOD, SCID, and NSG mice on a standard diet (**Fig. 1A**). Body composition analysis using ^{1}H-MRS showed that whole-body lean mass was significantly higher in NSG mice compared with WT mice (Fig. 1*B*). More striking was the difference in whole-body fat mass, which was 50–70% lower in NOD, SCID, and NSG mice compared with WT animals (Fig. 1*C*). Basal glucose levels were all lower in NOD, SCID, and NSG mice compared with WT mice, and SCID mice showed a significantly lower glucose level than NOD mice ($P = 0.008$ for SCID *vs.* NOD mice) (**Table 1**). In contrast, basal insulin levels were comparable among NOD, SCID, and NSG mice (Table 1).

Increased insulin sensitivity in NOD, SCID, and NSG mice

Following overnight food withdrawal, a 2 h hyperinsulinemic-euglycemic clamp was conducted to measure
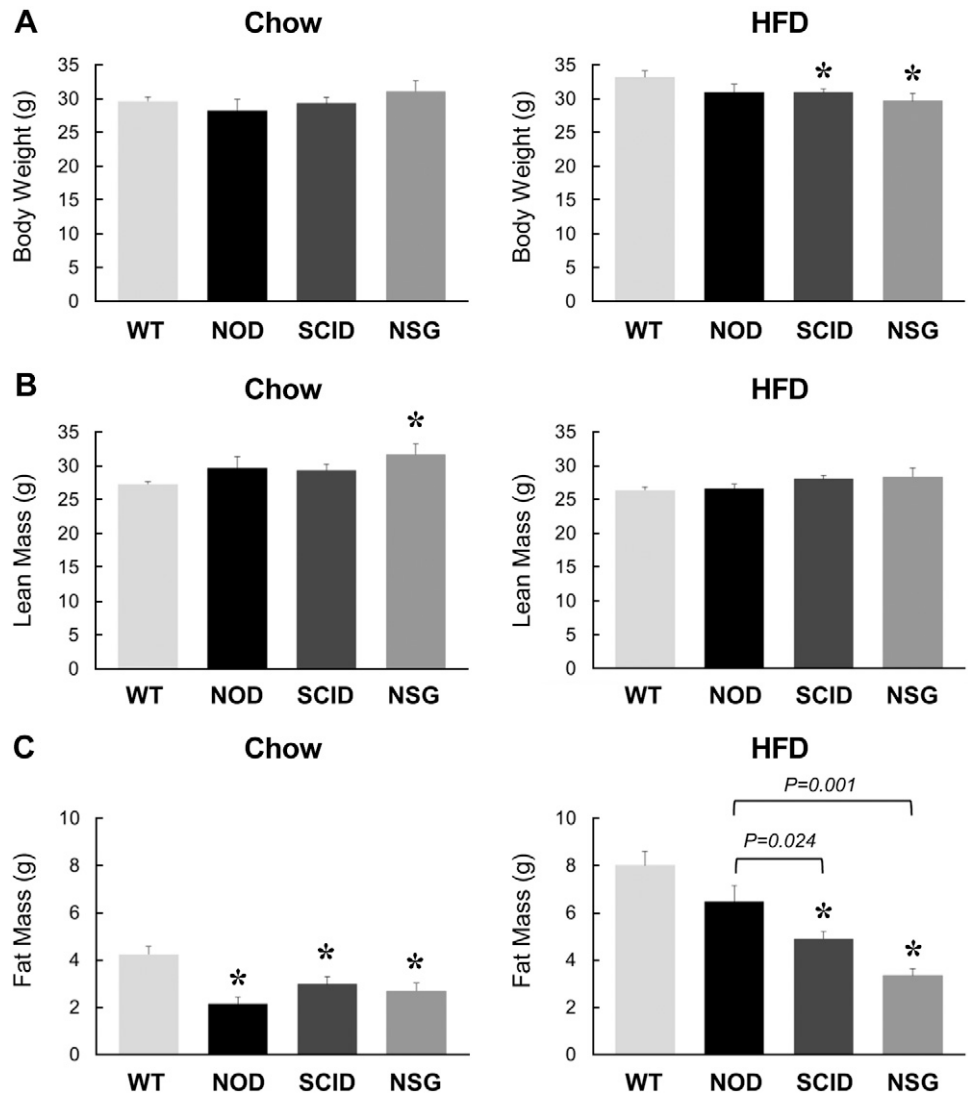
Figure 1. Metabolic profiles in 20-wk-old WT, NOD, SCID, and NSG mice fed a standard chow diet (n = 5–11 mice per group, left) or after 6 wk of an HFD (n = 6–15 mice per group, right). A) Body weights. B, C) Whole-body lean mass (B) and fat mass (C) measured using ^{1}H-MRS. *P < 0.05 vs. WT mice fed a respective diet.

insulin sensitivity and glucose metabolism in awake mice. During the clamp, plasma glucose levels were maintained at ~7 mM, and plasma insulin levels were raised to 2- to 3-fold over basal (~180 pM) in all groups of mice (Table 1). Steady-state glucose infusion rates to maintain euglycemia during clamps were significantly higher in NOD, SCID, and NSG mice compared with WT animals, suggesting that these mice are more insulin sensitive than C57BL/6J WT mice (**Fig. 2A**). Basal HGP rates did not differ between groups, and this is consistent with similar basal glucose levels in these mice (Fig. 2B). During clamp, insulin action caused a partial (~40%) suppression of HGP in WT mice, but insulin completely suppressed HGP in NOD, SCID, and NSG mice (Fig. 2C, D). Insulin-stimulated whole-body glucose turnover was measured using [3-^{3}H]glucose infusion during clamps and showed a 50% increase in SCID mice and a 2-fold increase in NOD and NSG mice compared with WT mice (**Fig. 3A**). Whole-body glycolysis and glycogen synthesis rates were also elevated in NOD, SCID, and NSG mice compared with WT mice (Fig. 3B, C). These data demonstrate that NOD, SCID, and NSG mice are more insulin sensitive than C57BL/6J WT animals.

Insulin-stimulated glucose uptake in individual organs was measured using a bolus injection of 2-[^{14}C]DG during clamps. Insulin-stimulated glucose uptake in skeletal muscle was increased by ~60% in NOD mice as compared with WT mice (**Fig. 4A**). Despite being more insulin sensitive, muscle glucose uptake in SCID and NSG mice did not differ mice WT mice. In fact, muscle glucose uptake tended to be lower in NSG mice compared with NOD mice (P = 0.054 vs. NOD mice; Fig. 4A). Insulin-stimulated glucose uptake in white adipose tissue was significantly increased in NOD, SCID, and NSG mice compared with WT mice (Fig. 4B). Glucose uptake in brown adipose tissue was significantly elevated in NOD and SCID mice, whereas brown fat glucose uptake tended to be higher in NSG mice compared with WT mice (Fig. 4C). Insulin-stimulated glucose uptake in the heart was significantly elevated in NOD mice and tended to be higher in SCID and NSG mice compared with WT mice (Fig. 4D).

Metabolic phenotypes in HFD-fed mice

To examine the effects of diet-induced obesity on glucose metabolism, separate cohorts of mice at 14 wk of age were fed an HFD for 6 wk. Following the HFD, WT and NOD mice became obese with comparable body weights and fat

TABLE 1. *Metabolic parameters at basal state and during hyperinsulinemic-euglycemic clamp in conscious mice*

Diet and genotype	Number	Basal state		Clamp period	
		Plasma glucose (mM)	Plasma insulin (pM)	Plasma glucose (mM)	Plasma insulin (pM)
Chow					
WT	6	8.2 ± 0.3	ND	7.4 ± 0.4	ND
NOD	5	5.9 ± 0.2*	64 ± 5	7.0 ± 0.4	168 ± 7
SCID	11	5.0 ± 0.2*	89 ± 15	6.7 ± 0.2	215 ± 27
NSG	6	5.2 ± 0.4*	73 ± 2	7.0 ± 0.4	164 ± 10
HFD					
WT	6	10.8 ± 0.7	ND	6.4 ± 0.5	ND
NOD	6	6.4 ± 0.8*	103 ± 17	6.4 ± 0.3	240 ± 22
SCID	15	5.2 ± 0.2*	109 ± 9	7.2 ± 0.4	255 ± 15
NSG	8	5.3 ± 0.4*	79 ± 2	7.3 ± 0.4	197 ± 11

ND, not determined. *$P < 0.05$ *vs.* WT.

mass (Fig. 1*A, C*). In contrast, SCID and NSG mice showed significantly lower body weights compared with WT mice after 6 wk of an HFD (Fig. 1*A*). This difference in diet-induced weight gain was largely due to 40–60% decreases in fat mass in SCID and NSG mice compared with WT mice (Fig. 1*C*). When compared to NOD mice, SCID and NSG mice also showed significantly lower fat mass after 6 wk of an HFD (Fig. 1*C*). Strikingly, NSG mice showed no difference in body weights before and after an HFD, demonstrating an impressive resistance to diet-induced obesity in these mice. Whole-body lean mass did not differ between groups (Fig. 1*B*).

After 6 wk of an HFD, WT mice developed fasting hyperglycemia (~10 mM), suggesting the onset of type 2 diabetes phenotypes in WT mice. Basal glucose levels were significantly lower in NOD, SCID, and NSG mice compared with WT mice, and in fact, NOD, SCID, and NSG mice showed euglycemia (5–6 mM) after 6 wk of an HFD (Table 1). Basal insulin levels also remained normal after 6 wk of an HFD and did not significantly differ from the chow-fed state in NOD, SCID, and NSG mice (Table 1). During clamp, plasma glucose levels were maintained at 6–7 mM, and plasma insulin levels were elevated to ~230 pM in all groups of mice (Table 1).

Protection from HFD-induced insulin resistance in NOD, SCID, and NSG mice

Following 6 wk of an HFD, WT mice developed insulin resistance with an ~20% decrease in the glucose infusion rate compared with chow-fed mice. Glucose infusion rates were significantly increased by 3- to 4-fold in HFD-fed NOD, SCID, and NSG mice compared with HFD-fed WT mice (Fig. 2*A*). In fact, the glucose infusion rates in the HFD-fed NSG mice were significantly increased compared with HFD-fed NOD mice. Despite differences in basal glucose levels, basal HGP rates did not differ between groups (Fig. 2*B*). Insulin caused a partial-to-complete suppression of HGP in all groups of mice, resulting in 60–90% suppression of HGP during insulin clamp (Fig. 2*C, D*). In contrast to comparable insulin action in the liver, insulin-stimulated whole-body glucose turnover was significantly increased by 2- to 3-fold in HFD-fed NOD, SCID, and NSG mice compared with HFD-fed WT mice (Fig. 3*A*).

This effect of increased insulin sensitivity was most impressive in NSG mice because glucose turnover tended to be higher in HFD-fed NSG mice compared with HFD-fed NOD mice (Fig. 3*A*). In fact, an HFD did not affect whole-body glucose turnover in NSG mice (287 ± 16 µmol/kg per minute in HFD-fed NSG mice *vs.* 291 ± 22 µmol/kg per minute in chow-fed NSG mice). Whole-body glycolysis and glycogen synthesis rates were also significantly elevated in HFD-fed NOD, SCID, and NSG mice compared with HFD-fed WT mice (Fig. 3*B, C*). Altogether, these results indicate that increased insulin sensitivity in HFD-fed NOD, SCID, and NSG mice was largely attributed to profound increases in whole-body glucose turnover and metabolic fluxes.

Insulin-stimulated glucose uptake in skeletal muscle was significantly increased in HFD-fed SCID and NSG mice compared with HFD-fed WT mice (Fig. 4*A*). Glucose uptake in white adipose tissue was also significantly elevated in HFD-fed SCID and NSG mice compared with HFD-fed WT mice (Fig. 4*B*). Glucose uptake in brown adipose tissue was only increased significantly in HFD-fed NSG mice compared with HFD-fed WT mice (Fig. 4*C*). Insulin-stimulated glucose uptake in the heart was elevated in HFD-fed NOD, SCID, and NSG mice compared with HFD-fed WT mice (Fig. 4*D*).

Effects of an HFD on energy balance

To determine the potential mechanism of altered weight gain in response to an HFD in NOD, SCID, and NSG mice, we performed a longitudinal analysis of body composition and energy balance using TSE Systems Incorporated metabolic cages. During 5 wk of an HFD, NOD mice became obese with a 2.5-fold increase in whole-body fat mass (3.2 ± 0.2 g at baseline *vs.* 7.3 ± 0.7 g after 5 wk) (**Fig. 5A, B**). In contrast, diet-induced weight gain was noticeably blunted in SCID and NSG mice, and whole-body fat mass remained profoundly lower in SCID and NSG mice compared with NOD mice over the course of 5 wk of an HFD (Fig. 5*B*). Consistent with previous observations, the most impressive effect of resistance to diet-induced obesity was shown by NSG mice whose fat mass was minimally affected by 5 wk of an HFD (2.3 ± 0.2 g at baseline *versus* 3.6 ± 0.2 g after 5 wk) (Fig. 5*B*). To further evaluate these mice, we followed the changes in body composition during 12 wk of an HFD

Figure 2. A 2 h hyperinsulinemic-euglycemic clamp was performed in 20-wk-old WT, NOD, SCID, and NSG mice fed a standard chow diet ($n = 5$–11 mice per group, left) or after 6 wk of an HFD ($n = 6$–15 mice per group, right). *A*) Steady-state glucose infusion rates during clamps. *B, C*) HGP at basal state and (*B*) during insulin-stimulated state (clamp) (*C*). *D*) Hepatic insulin action expressed as insulin-mediated percent suppression of basal HGP. $*P < 0.05$ *vs.* WT mice fed a respective diet.
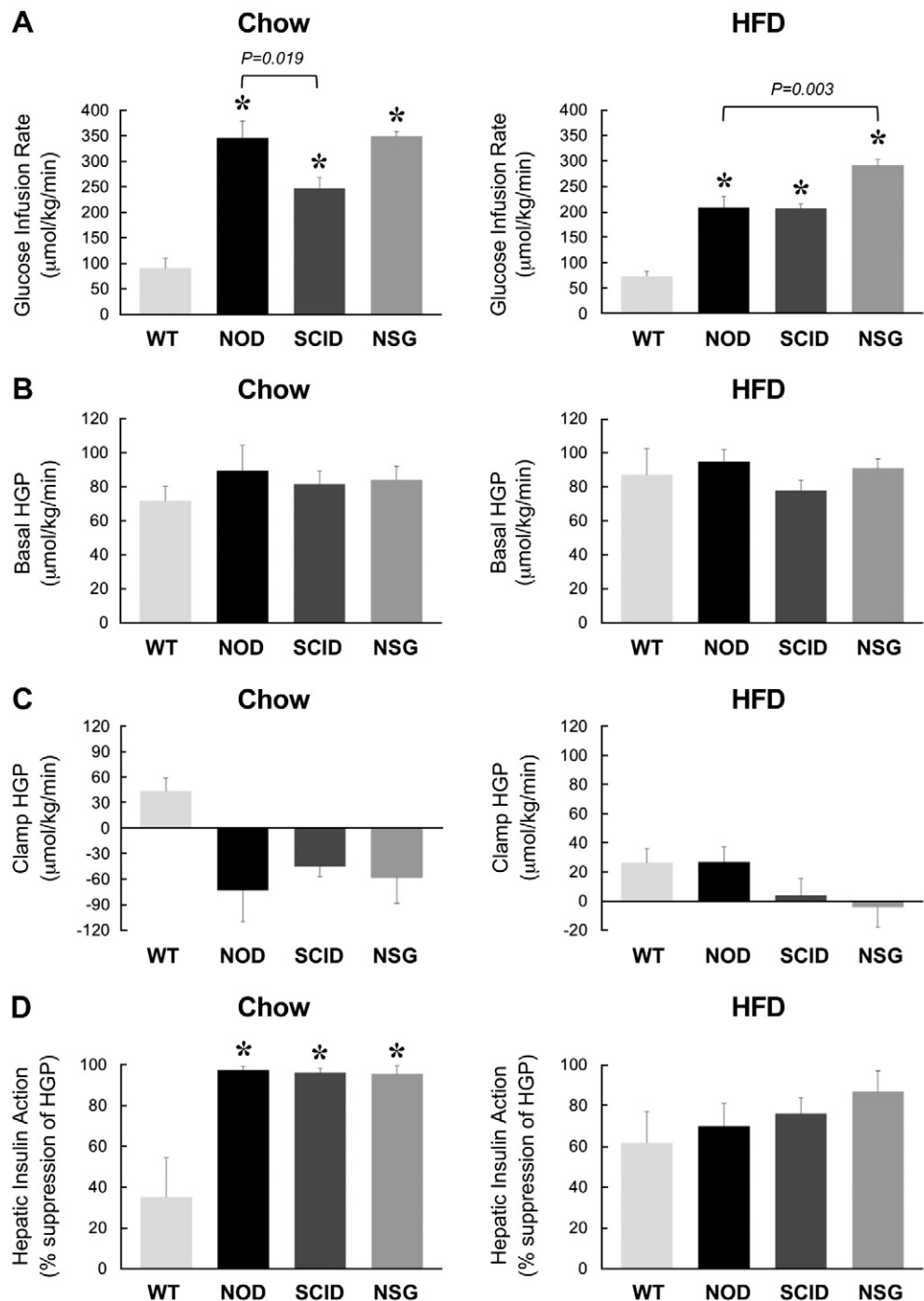
and found that NSG mice were remarkably resistant to diet-induced obesity even during the chronic HFD feeding (2.5 ± 0.2 g at baseline, 5.1 ± 0.6 g after 8 wk of an HFD, and 5.8 ± 0.6 g after 12 wk of an HFD) (Fig. 5*C*).

To determine the mechanism of resistance to diet-induced obesity, we performed a 3 d analysis of energy balance in NOD, SCID, and NSG mice fed chow or an HFD using metabolic cages. Daily food intake was not significantly different in any of the groups on either diet (Fig. 5*D*). On chow diet, oxygen consumption (V_{O_2},) was significantly reduced in NSG mice compared with NOD mice (Fig. 5*E*). After 6 wk of an HFD, V_{O_2}, was significantly higher in SCID mice compared with NOD mice. Interestingly, the HFD caused a significant increase in V_{O_2} in SCID and NSG mice compared with the chow-fed state, but this HFD effect was not shown in NOD mice (Fig. 5*E*). Carbon dioxide production (V_{CO_2}) during the chow-fed state was significantly lower in NSG mice compared with NOD mice (Fig. 5*F*). After an HFD, the V_{CO_2} rate was significantly higher in SCID mice compared with NOD mice. In contrast to the effect on V_{O_2} an HFD significantly reduced V_{CO_2} selectively in NOD mice, whereas an HFD did not affect V_{CO_2} in SCID or NSG mice (Fig. 5*F*). RERs were significantly elevated in SCID mice compared with NOD
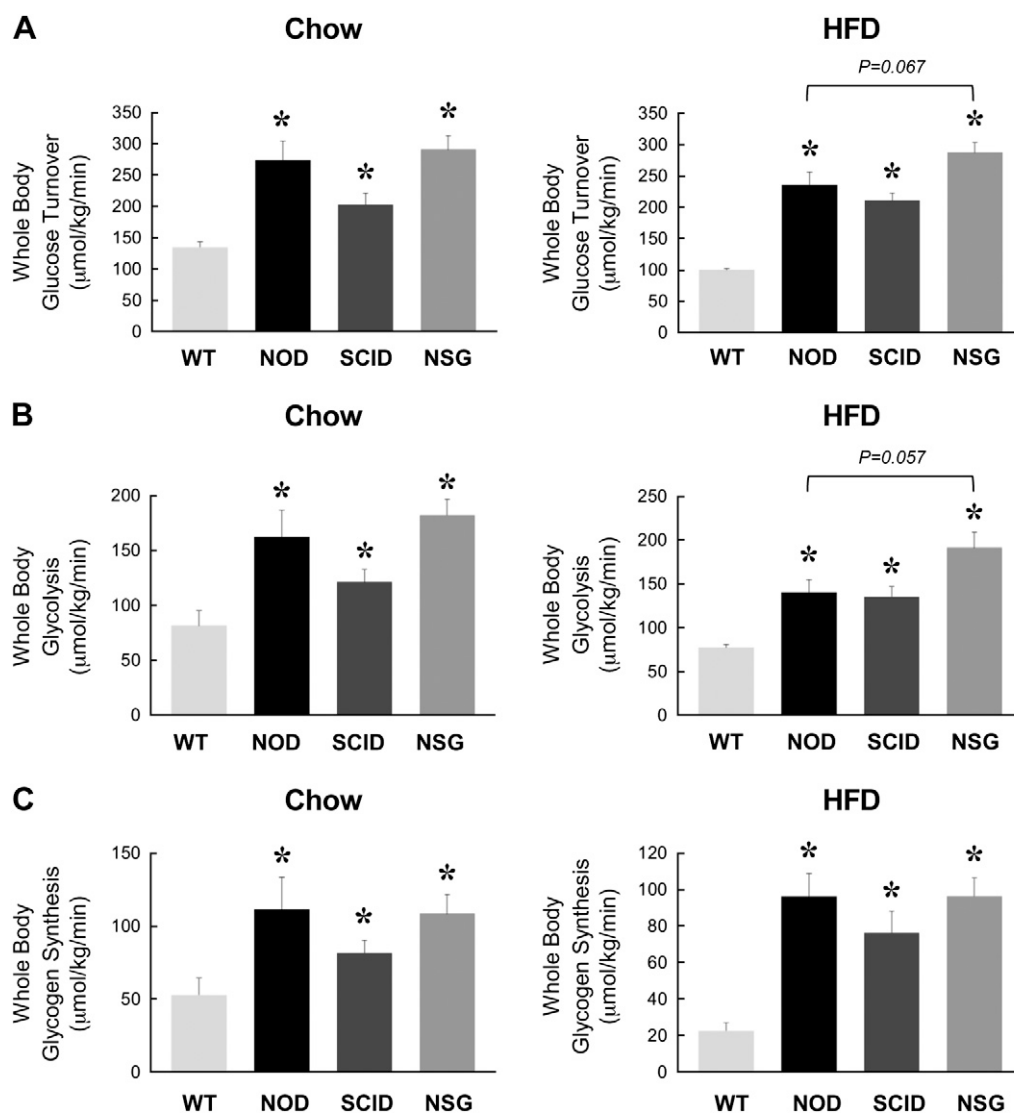
The FASEB Journal · www.fasebj.org

Figure 3. Insulin-stimulated whole-body glucose turnover (*A*), glycolysis (*B*), and glycogen synthesis (*C*) during a 2 h hyperinsulinemic-euglycemic clamp in 20-wk-old WT, NOD, SCID, and NSG mice fed a standard chow diet (*n* = 5–11 mice per group, left) or after 6 wk of an HFD (*n* = 6–15 mice per group, right). *$P < 0.05$ *vs.* WT mice fed a respective diet.

mice fed chow or an HFD (Fig. 5*G*). RER tended to increase in HFD-fed NSG mice compared with HFD-fed NOD mice, but this difference did not reach statistical significance (*P* = 0.088). As expected, high-fat feeding lowered RERs toward 0.78 in all groups of mice, indicating HFD-mediated utilization of fatty acids (Fig. 5*G*). Consistent with the changes in energy expenditure, physical activity was only increased significantly in SCID mice mice compared with NOD mice fed chow or an HFD (Fig. 5*H*).

Because SCID mice showed the most impressive and consistent changes in energy expenditure and physical activity, we performed an additional metabolic cage study in a separate cohort of SCID and C57BL/6J WT mice fed chow or an HFD for 6 wk. Compared with WT mice, SCID mice showed significant increases in daily food intake during chow or HFD feeding (**Fig. 6*A***). Interestingly, *V*o₂ rates were significantly reduced in SCID mice during the chow diet, but these rates were significantly increased in SCID mice during the HFD compared with WT mice (Fig. 6*B, C*). Energy expenditure rates were also reduced in

chow-fed SCID mice but were increased in HFD-fed SCID mice compared with WT mice fed respective diets (Fig. 6*D*). Physical activity was also significantly lower in chow-fed SCID mice but tended to remain higher in HFD-fed SCID mice compared with WT mice fed respective diets (Fig. 6*E*).

DISCUSSION

Despite widespread use of NOD and NOD-SCID mice as models of type 1 diabetes and islet graft transplantation, the metabolic states of these mice have not been fully characterized. This is important because underlying changes in glucose and lipid metabolism may affect the application and utility of these mouse models. Also, understanding their basal metabolic states and their response to diet-induced obesity will enhance data interpretation following subsequent experimental manipulations. Our results indicate that NOD mice are inherently leaner than
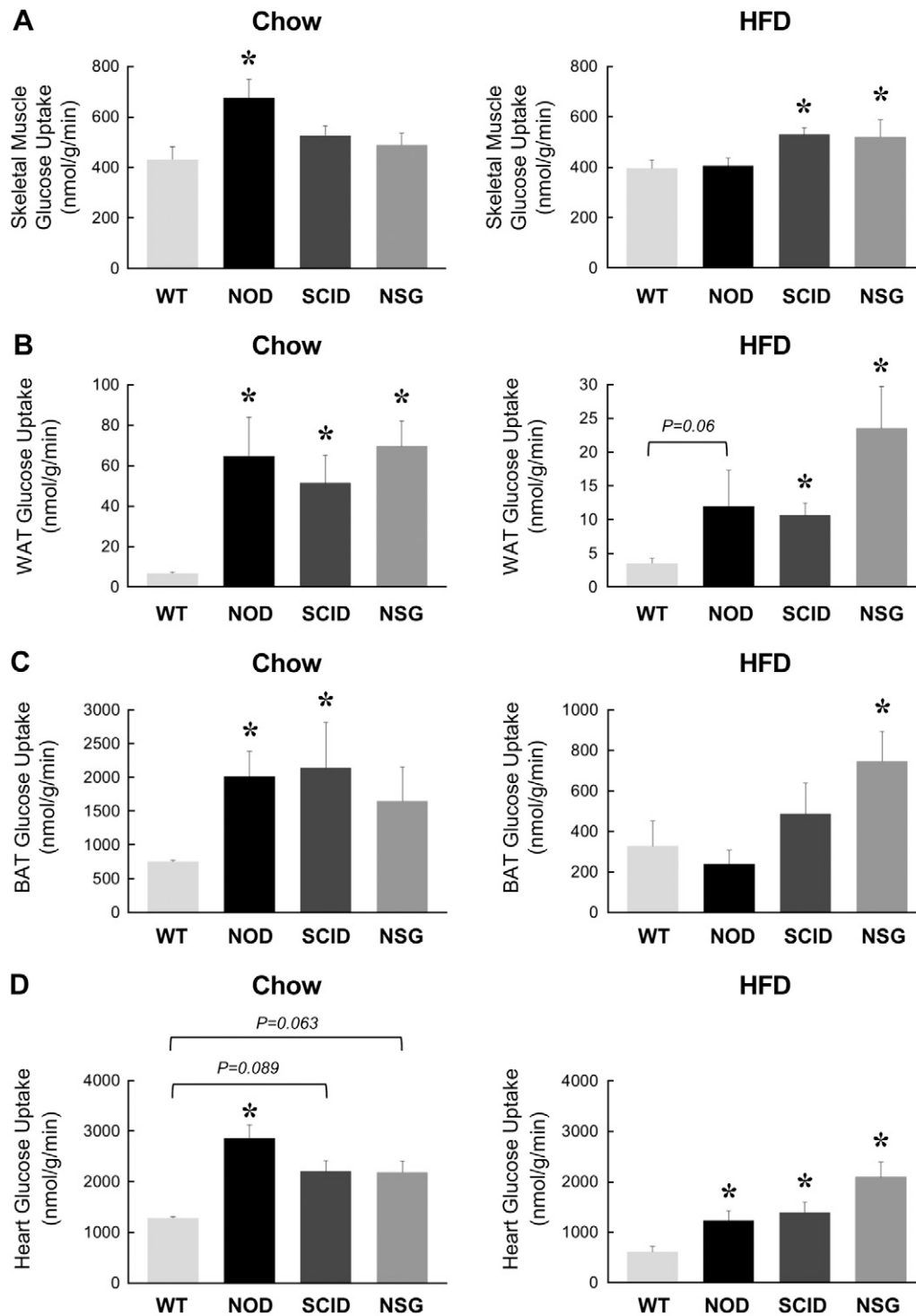
Figure 4. Insulin-stimulated glucose uptake in individual organs was measured using a bolus injection of 2-[^{14}C]DG during hyperinsulinemic-euglycemic clamp in 20-wk-old WT, NOD, SCID, and NSG mice fed a standard chow diet (n = 5–11 mice per group, left) or after 6 wk of an HFD (n = 6–15 mice per group, right). *A*) Skeletal muscle glucose uptake (*gastrocnemius*). *B*) Glucose uptake in epidydimal white adipose tissue (WAT). *C*) Glucose uptake in intrascapular brown adipose tissue (BAT). *D*) Myocardial glucose uptake. *P < 0.05 *vs.* WT mice fed a respective diet.

C57BL/6J WT mice, and this was mostly due to ~50% less whole-body fat mass in NOD mice. NOD mice also showed lower fasting glucose levels, and these mice were profoundly more insulin sensitive than WT mice. Because whole-body adiposity is inversely correlated with insulin sensitivity, lower fat mass in NOD mice may partly explain

2- to 3-fold increases in whole-body glucose turnover and hepatic insulin action in these mice compared with WT mice. All insulin-responsive organs were more insulin sensitive because insulin-stimulated glucose uptake rates in skeletal muscle, white and brown adipose tissue, and the heart were significantly increased in NOD mice compared
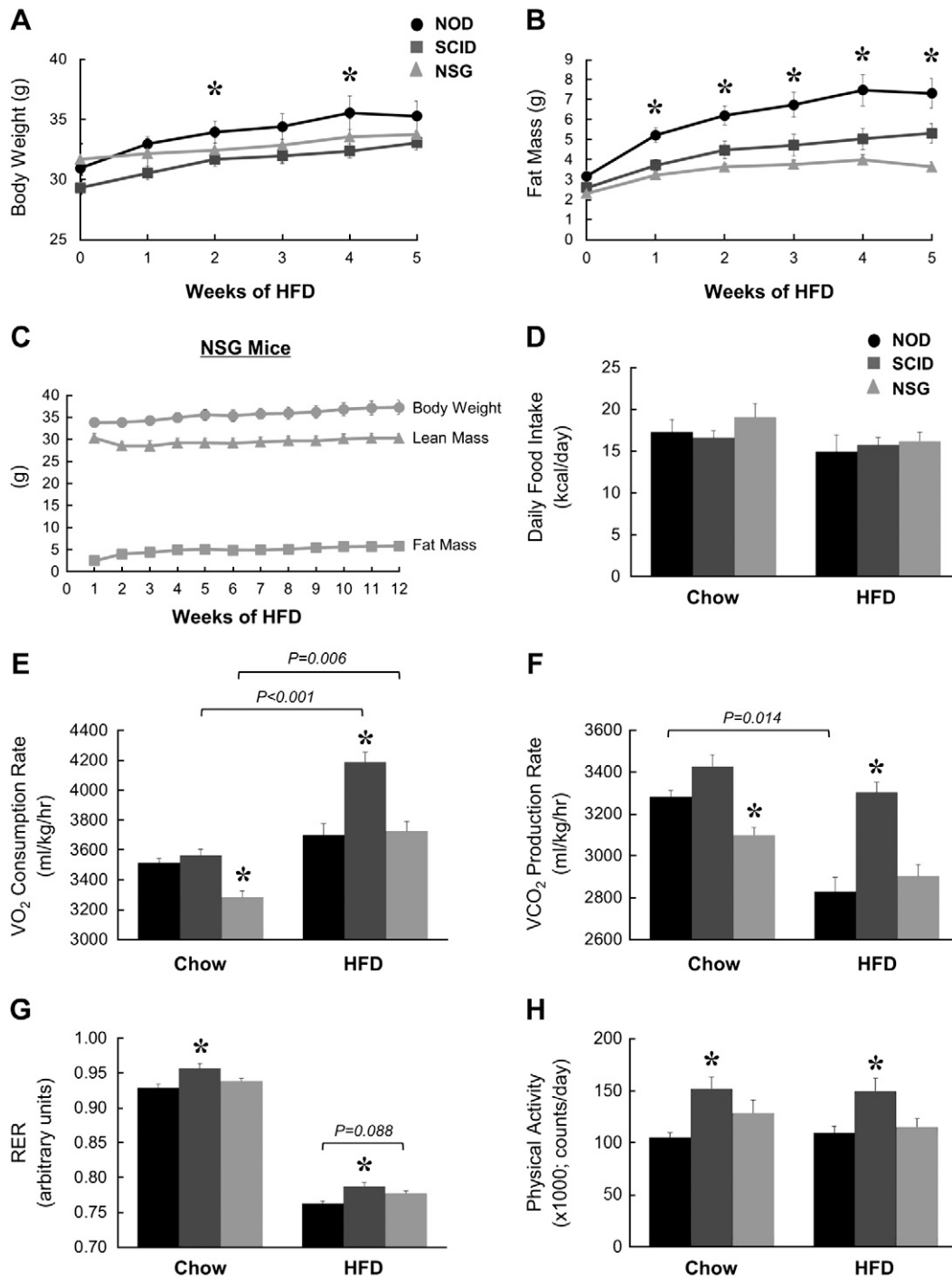
Figure 5. Indirect calorimetry was performed using metabolic cages for 3 d in NOD, SCID, and NSG mice fed a chow diet or an HFD (*n* = 5 per group). *A*) Body weights. *B*) Whole-body fat mass was measured using ^{1}H-MRS during 5 wk of an HFD. *C*) Male NSG mice were fed an HFD for 12 wk, and body weight, whole-body fat mass, and lean mass were measured weekly using ^{1}H-MRS. *D*) Average daily food intake in mice. *E*) V_{O_2}, rates. *F*) V_{CO_2} rates. *G*) RER based on V_{O_2} and V_{CO_2} rates. *H*) Physical activity measured as total beam break counts. *P < 0.05 *vs.* NOD mice fed a respective diet.

with WT mice. It is important to note that NOD mice were leaner despite a 10-fold increase in glucose uptake into white adipose tissue compared with WT mice, suggesting that *de novo* lipogenesis was likely not increased in these mice. These metabolic effects of NOD mice are a stark contrast to what we had previously found in NOD-*Ins2*[Akita] mice, an insulin-deficient model of type 1 diabetes (26). Despite a modest reduction in whole-body fat mass,

NOD-*Ins2*[Akita] mice are severely insulin resistant with marked reductions in skeletal muscle glucose metabolism and hepatic insulin action (26). The fact that lower adiposity in both NOD and NOD-*Ins2*[Akita] mice, which may be due to reduced insulin levels, is associated with opposing effects on insulin action suggests that other factors, possibly related to autoimmunity, may be responsible for enhanced insulin sensitivity in NOD mice.
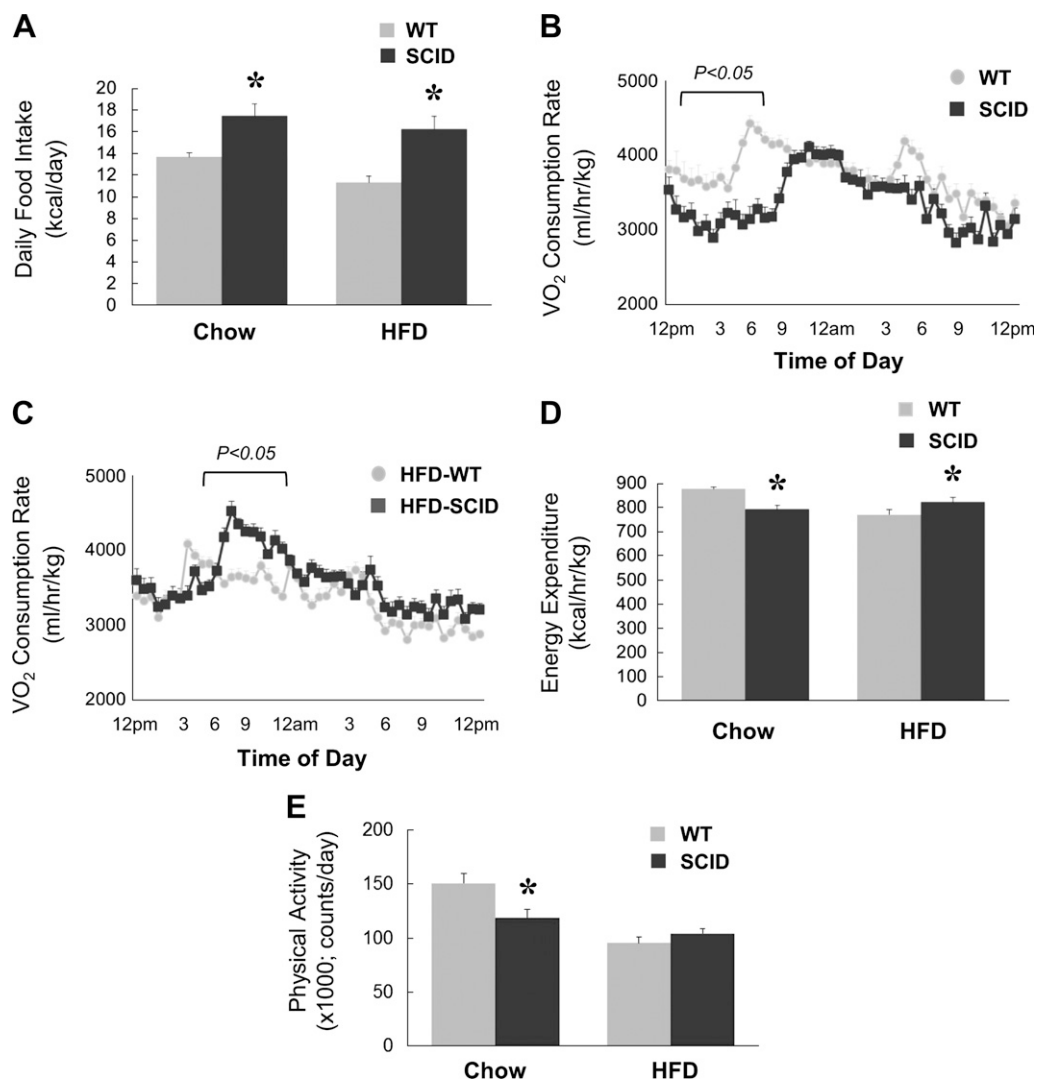
Figure 6. Indirect calorimetry was performed using metabolic cages for 3 d in an additional cohort of SCID and WT mice fed chow or an HFD for 6 wk (*n* = 6 per group). *A*) Average daily food intake in mice. *B*) A 3 d average of instantaneous Vo_2 rates measured for 24 h in chow-fed mice. *C*) A 3 d average of instantaneous Vo_2 rates measured for 24 h in HFD-fed mice. *D*) Energy expenditure rates calculated as kilocaloriies per hour per kilogram body weight in mice. *E*) Physical activity measured as total beam break counts. *P < 0.05 *vs.* WT mice fed a respective diet.

After 6 wk of an HFD, NOD mice became obese, although they tended to be less obese than WT mice. However, dramatic effects on insulin sensitivity were observed because HFD-fed NOD mice remained significantly more insulin sensitive than HFD-fed WT mice. This was largely due to more than a 2-fold increase in whole-body glucose turnover in HFD-fed NOD mice because hepatic insulin action did not differ between NOD and WT mice after high-fat feeding. Surprisingly, enhanced glucose turnover in HFD-fed NOD mice did not result from increased muscle glucose metabolism. In fact, the only organs showing increased glucose uptake were the heart and white adipose tissue. These data indicate that selective organs remained insulin sensitive after an HFD, and such effects were not dependent on adiposity changes in NOD mice.

On a standard chow diet, SCID mice are also leaner than WT mice due to 30% less whole-body fat mass. SCID mice also showed lower fasting glucose levels compared with WT mice, and in fact, their plasma glucose levels were significantly lower than the NOD mice. The SCID mice were also more insulin sensitive than WT mice, and this was due to increased whole-body glucose turnover and hepatic insulin action in SCID mice compared with WT mice. The SCID mice also showed increased glucose metabolism in white and brown adipose tissue as well as the heart, but their effects were less pronounced than those observed in NOD mice. These data indicate that lymphocyte deficiency did not further enhance insulin action on the NOD background.

On the other hand, lymphocyte deficiency from the SCID mutation resulted in much more dramatic effects on the NOD background after high-fat feeding. Following 6 wk of an HFD, SCID mice gained significantly less fat mass than both WT and NOD mice. In fact, our longitudinal assessment of changes in whole-body fat mass using ^{1}H-MRS found that SCID mice gained significantly less fat mass than NOD mice over the course of 5 wk of an HFD.

Recombination activating gene 1 *(Rag1),* involved in somatic DNA rearrangement and V(D)J recombination, plays an important role in the development of B- and T-cell lymphocytes, and *Rag1*-deficient mice were shown to have no mature B- and T-cell lymphocytes (27). In that regard, Winer *et al.* (20) recently found that C57BL/6J-*Rag1^null* mice gained more body weight and fat mass and became more glucose intolerant after an HFD. These metabolic effects of RAG1 deficiency on a C57BL/6 strain are completely opposite to our observation in SCID mice on the NOD strain despite both mouse strains lacking B- and T-cell lymphocytes. To that end, HFD-fed SCID mice remained more insulin sensitive than HFD-fed WT mice, and this was due to significant increases in muscle and adipose tissue glucose metabolism in HFD-fed SCID mice. Thus, these findings indicate that the NOD strain background is able to completely reverse the metabolic effects of lymphocyte deficiency, and further studies are needed to delineate the underlying mechanism responsible for this interesting observation.

Our metabolic cage study showed that the effect of the *scid* mutation on the NOD strain rendering mice partially resistant to diet-induced obesity may be largely due to increased energy expenditure and physical activity in SCID mice. To that end, both Vo_2 rate and Vco_2 rate were increased by ~15% in HFD-fed SCID mice compared with HFD-fed NOD mice. These effects were consistent with a 36% increase in physical activity in HFD-fed SCID mice compared with HFD-fed NOD mice. Additionally, whereas an HFD reduced the Vco_2 rate in NOD mice, possibly reflecting mitochondrial dysfunction in response to diet-induced obesity (28), SCID mice were completely resistant to such effects of an HFD on the Vco_2 rate. Thus, these results suggest that the absence of B and T lymphocytes may protect mitochondrial function from the deleterious effects of diet-induced obesity in mice.

Although the SCID mice were partially resistant to diet-induced obesity and insulin resistance, the most impressive metabolic effects in response to an HFD were shown by NSG mice. Over the course of 5 and 12 wk of an HFD, NSG mice gained minimal fat mass and remained significantly leaner than NOD or WT mice. In contrast to SCID mice, such resistance to diet-induced weight gain in NSG mice was not associated with any changes in energy expenditure or physical activity compared with NOD mice. Daily food intake also did not differ between NSG and NOD mice. HFD-fed NSG mice also remained highly insulin sensitive with glucose uptake rates in skeletal muscle, the heart, and adipose tissue that rival those in chow-fed mice. Our findings are in stark contrast to Behan *et al.* (24) who recently showed that NSG mice became obese while remaining glucose tolerant when these mice were weaned onto an HFD. However, it is important to note that in the study by Behan *et al.* (24), obesity effects were more pronounced in female NSG mice, whereas male NSG mice gained minimal body weight at 12 wk of age. Thus, our discordant findings on the effects of an HFD on obesity may reflect gender-specific effects in NSG mice. In fact, their findings of protective effects against diet-induced insulin resistance in NSG mice are consistent with our results. Additionally, our findings suggest that NSG mice were protected from HFD-induced insulin resistance due to their resistance to weight gain during high-fat feeding. The mechanism by which NSG mice do not become obese without changes in energy balance requires further studies.

Overall, we provide a comprehensive metabolic characterization of NOD, SCID, and NSG mice fed chow or an HFD. Our results indicate that NOD mice are more insulin sensitive than B6 WT mice, and the *scid* mutation on the NOD strain rescues HFD-mediated decline in energy expenditure resulting in less obesity after an HFD. Finally, male NSG mice are completely resistant to diet-induced obesity and insulin resistance. Thus, our findings support an important role of genetic background, lymphocytes, and cytokine signaling in the regulation of diet-induced obesity and insulin resistance. **FJ**

REFERENCES

1. Leiter, E. H., Prochazka, M., and Coleman, D. L. (1987) The nonobese diabetic (NOD) mouse. *Am. J. Pathol.* **128**, 380–383
2. Atkinson, M. A., and Leiter, E. H. (1999) The NOD mouse model of type 1 diabetes: as good as it gets? *Nat. Med.* **5**, 601–604
3. Bosma, M. J., and Carroll, A. M. (1991) The SCID mouse mutant: definition, characterization, and potential uses. *Annu. Rev. Immunol.* **9**, 323–350
4. Christianson, S. W., Shultz, L. D., and Leiter, E. H. (1993) Adoptive transfer of diabetes into immunodeficient NOD-*scid/scid* mice. Relative contributions of CD4^{+} and CD8^{+} T-cells from diabetic versus prediabetic NOD.NON-*Thy-1^a* donors. *Diabetes* **42**, 44–55
5. Peterson, J. D., and Haskins, K. (1996) Transfer of diabetes in the NOD-*scid* mouse by CD4 T-cell clones. Differential requirement for CD8 T-cells. *Diabetes* **45**, 328–336
6. Van der Loo, J. C., Hanenberg, H., Cooper, R. J., Luo, F. Y., Lazaridis, E. N., and Williams, D. A. (1998) Nonobese diabetic/severe combined immunodeficiency (NOD/SCID) mouse as a model system to study the engraftment and mobilization of human peripheral blood stem cells. *Blood* **92**, 2556–2570
7. Prochazka, M., Gaskins, H. R., Shultz, L. D., and Leiter, E. H. (1992) The nonobese diabetic *scid* mouse: model for spontaneous thymomagenesis associated with immunodeficiency. *Proc. Natl. Acad. Sci. USA* **89**, 3290–3294
8. Gaber, A. O., Fraga, D., Kotb, M., Lo, A., Sabek, O., and Latif, K. (2004) Human islet graft function in NOD-SCID mice predicts clinical response in islet transplant recipients. *Transplant. Proc.* **36**, 1108–1110
9. Greiner, D. L., Brehm, M. A., Hosur, V., Harlan, D. M., Powers, A. C., and Shultz, L. D. (2011) Humanized mice for the study of type 1 and type 2 diabetes. *Ann. N. Y. Acad. Sci.* **1245**, 55–58
10. Boden, G., and Shulman, G. I. (2002) Free fatty acids in obesity and type 2 diabetes: defining their role in the development of insulin resistance and beta-cell dysfunction. *Eur. J. Clin. Invest.* **32**(Suppl 3), 14–23
11. Sell, H., Habich, C., and Eckel, J. (2012) Adaptive immunity in obesity and insulin resistance. *Nat. Rev. Endocrinol.* **8**, 709–716

12. Shi, H., Kokoeva, M. V., Inouye, K., Tzameli, I., Yin, H., and Flier, J. S. (2006) TLR4 links innate immunity and fatty acid-induced insulin resistance. *J. Clin. Invest.* 116, 3015–3025

13. Dandona, P., Aljada, A., and Bandyopadhyay, A. (2004) Inflammation: the link between insulin resistance, obesity and diabetes. *Trends Immunol.* 25, 4–7

14. Pickup, J. C., Chusney, G. D., Thomas, S. M., and Burt, D. (2000) Plasma interleukin-6, tumour necrosis factor alpha and blood cytokine production in type 2 diabetes. *Life Sci.* 67, 291–300

15. Weisberg, S. P., McCann, D., Desai, M., Rosenbaum, M., Leibel, R. L., and Ferrante, A. W., Jr. (2003) Obesity is associated with macrophage accumulation in adipose tissue. *J. Clin. Invest.* 112, 1796–1808

16. Xu, H., Barnes, G. T., Yang, Q., Tan, G., Yang, D., Chou, C. J., Sole, J., Nichols, A., Ross, J. S., Tartaglia, L. A., and Chen, H. (2003) Chronic inflammation in fat plays a crucial role in the development of obesity-related insulin resistance. *J. Clin. Invest.* 112, 1821–1830

17. Olefsky, J. M., and Glass, C. K. (2010) Macrophages, inflammation, and insulin resistance. *Annu. Rev. Physiol.* 72, 219–246

18. Hong, E. G., Ko, H. J., Cho, Y. R., Kim, H. J., Ma, Z., Yu, T. Y., Friedline, R. H., Kurt-Jones, E., Finberg, R., Fischer, M. A., Granger, E. L., Norbury, C. C., Hauschka, S. D., Philbrick, W. M., Lee, C. G., Elias, J. A., and Kim, J. K. (2009) Interleukin-10 prevents diet-induced insulin resistance by attenuating macrophage and cytokine response in skeletal muscle. *Diabetes* 58, 2525–2535

19. Stolarczyk, E., Vong, C. T., Perucha, E., Jackson, I., Cawthorne, M. A., Wargent, E. T., Powell, N., Canavan, J. B., Lord, G. M., and Howard, J. K. (2013) Improved insulin sensitivity despite increased visceral adiposity in mice deficient for the immune cell transcription factor T-bet. *Cell Metab.* 17, 520–533

20. Winer, S., Chan, Y., Paltser, G., Truong, D., Tsui, H., Bahrami, J., Dorfman, R., Wang, Y., Zielenski, J., Mastronardi, F., Maezawa, Y., Drucker, D. J., Engleman, E., Winer, D., and Dosch, H. M. (2009) Normalization of obesity-associated insulin resistance through immunotherapy. *Nat. Med.* 15, 921–929

21. Feng, B., Jiao, P., Nie, Y., Kim, T., Jun, D., van Rooijen, N., Yang, Z., and Xu, H. (2011) Clodronate liposomes improve metabolic profile and reduce visceral adipose macrophage content in diet-induced obese mice. *PLoS One* 6, e24358

22. Ito, M., Hiramatsu, H., Kobayashi, K., Suzue, K., Kawahata, M., Hioki, K., Ueyama, Y., Koyanagi, Y., Sugamura, K., Tsuji, K., Heike, T., and Nakahata, T. (2002) NOD/SCID/γ(c)(null) mouse: an excellent recipient mouse model for engraftment of human cells. *Blood* 100, 3175–3182

23. Shultz, L. D., Lyons, B. L., Burzenski, L. M., Gott, B., Chen, X., Chaleff, S., Kotb, M., Gillies, S. D., King, M., Mangada, J., Greiner, D. L., and Handgretinger, R. (2005) Human lymphoid and myeloid cell development in NOD/LtSz-scid IL2R gamma null mice engrafted with mobilized human hemopoietic stem cells. *J. Immunol.* 174, 6477–6489

24. Behan, J. W., Ehsanipour, E. A., Sheng, X., Pramanik, R., Wang, X., Hsieh, Y. T., Kim, Y. M., and Mittelman, S. D. (2013) Activation of adipose tissue macrophages in obese mice does not require lymphocytes. *Obesity (Silver Spring)* 21, 1380–1388

25. Kim, J. K. (2009) Hyperinsulinemic-euglycemic clamp to assess insulin sensitivity in vivo. *Methods Mol. Biol.* 560, 221–238

26. Hong, E. G., Jung, D. Y., Ko, H. J., Zhang, Z., Ma, Z., Jun, J. Y., Kim, J. H., Sumner, A. D., Vary, T. C., Gardner, T. W., Bronson, S. K., and Kim, J. K. (2007) Nonobese, insulin-deficient Ins2[Akita] mice develop type 2 diabetes phenotypes including insulin resistance and cardiac remodeling. *Am. J. Physiol. Endocrinol. Metab.* 293, E1687–E1696

27. Mombaerts, P., Iacomini, J., Johnson, R. S., Herrup, K., Tonegawa, S., and Papaioannou, V. E. (1992) RAG-1-deficient mice have no mature B and T lymphocytes. *Cell* 68, 869–877

28. Parish, R., and Petersen, K. F. (2005) Mitochondrial dysfunction and type 2 diabetes. *Curr. Diab. Rep.* 5, 177–183
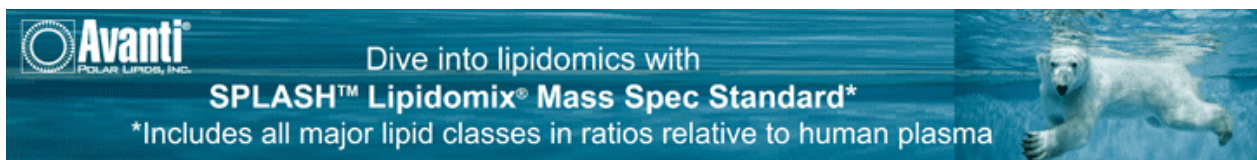
Genetic ablation of lymphocytes and cytokine signaling in nonobese diabetic mice prevents diet-induced obesity and insulin resistance

Randall H. Friedline, Hwi Jin Ko, Dae Young Jung, et al.

References	This article cites 27 articles, 8 of which can be accessed free at: http://www.fasebj.org/content/30/3/1328.full.html#ref-list-1
Subscriptions	Information about subscribing to *The FASEB Journal* is online at http://www.faseb.org/The-FASEB-Journal/Librarian-s-Resources.aspx
Permissions	Submit copyright permission requests at: http://www.fasebj.org/site/misc/copyright.xhtml
Email Alerts	Receive free email alerts when new an article cites this article - sign up at http://www.fasebj.org/cgi/alerts